IEEE Access
Multidisciplinary | Rapid Review | Open Access Journal

Received July 5, 2021, accepted July 7, 2021, date of publication July 12, 2021, date of current version July 20, 2021.

Digital Object Identifier 10.1109/ACCESS.2021.3096187

A Novel Varactorless Tuning Technique for Clapp VCO Design Using Tunable Negative Capacitor to Increase Frequency-Tuning Range

DANG-AN NGUYEN[1], (Graduate Student Member, IEEE), AND CHULHUN SEO[2], (Senior Member, IEEE)

[1]Department of Information Communication, Materials, and Chemistry Convergence Technology, Soongsil University, Seoul 156-743, South Korea
[2]School of Electronic Engineering, Soongsil University, Seoul 156-743, South Korea

Corresponding author: Chulhun Seo (chulhun@ssu.ac.kr)

This work was supported in part by the National Research Foundation of Korea (NRF) through a grant through the Ministry of Education under Grant NRF-2017R1D1A1B05032539, and in part by the National Research Foundation of Korea (NRF) through a grant through the Korean Government (MSIP) under Grant NRF-2017R1A5A1015596.

ABSTRACT In this paper, a varactorless frequency-tuning method for Clapp voltage-controlled oscillator (VCO) design is proposed aiming at increasing frequency-tuning range (FTR) in comparison with the conventional varactor-based counterpart. The proposed structure uses a tunable non-Foster (negative) capacitor (TNC) to sweep oscillation frequency instead of a varactor. The analytical demonstration points that total tuning dynamic (TTD) qualitatively representing FTR is traditionally limited to varactor's tuning dynamic (TD); while the TNC-based VCO can exhibit very-high TTD, at least over TNC's TD capacity, if the maximum negative capacitance is appropriately designed, which can tolerate the TD requirement on the tuning component for wideband operation. Circuit realization of TNC is based on a grounded negative impedance inverter (NII) with cross-coupled transistors whose gate voltage controls capacitance. A simulation script using a real discrete transistor model with the realized TNC shows that FTR can be covered with TTD of 2.46 units while the TD of the non-Foster tuning component is only 1.32 units, validating the advantageous operation as well as practical realization possibility of the proposed VCO. In addition, phase noise performance is remained below −100 dBc/Hz for every tuning voltages at 1 MHz offset frequency, while figure of merit comprising FTR effect (FOMT) can be achieved in range of 140-180, which is similar to the existing state-of-the-art VCOs.

INDEX TERMS JFET, colpitt and clapp VCOs, negative impedance inverter, non-foster capacitor, negative resistance.

I. INTRODUCTION

The LC oscillators are the essential radio frequency (RF) front-end and back-end building blocks in modern communication systems. They are widely generated from voltage-controlled oscillators (VCOs) injected in phase lock loops (PLLs) to up-convert or down-convert signals. There are several different LC VCO topologies, but Copitts and Clapp topologies have attracted more attention in both research and deployment [1]–[4].

The commonly used tuning method in LC-VCOs is based on varying the LC-tank capacitance. With the growth of wireless broadband and multiband communication systems, a high frequency-tuning range (FTR) of VCOs are required to cover the required frequency bands. Moreover, wideband VCOs are also demanded to compensate for process and temperature variations producing a stable-frequency oscillation in PLL applications [5]. However, the FTR of the conventional LC Clapp VCOs with the varactor-based tuning technique is always limited due to the capacitance ratio C_{max}/C_{min}, referred as ''tuning dynamic (TD)'', of the varactor.

One of the most effective methods that can be applied to the Clapp VCOs to achieve wide FTR is to use a switched-capacitor array bank or a varactor-combined binary switched capacitor array structure [6], [7]. However, one of the serious and practical issues in these structures is the large variations in the tuning sensitivities since the structure

The associate editor coordinating the review of this manuscript and approving it for publication was Chaitanya U. Kshirsagar.

becomes large. In addition, the parasitics from each capacitor and switches cause ineffective performance at higher frequencies [8]. Some of varactorless tuning techniques are also carried out to enhance FTR such as using a tunable negative inductor [5], a transconductance-tuned resonant tank [9], or voltage-controlled inductors [10]. Nevertheless, these VCOs always require high-TD tuning components for their wideband operation leading to a severe requirement on the tuning-range capacity of those controlling elements.

Non-Foster elements are typically known as negative capacitors, or negative inductors which exhibit negative-slope reactance with frequency [11]. Due to their non-natural response, these components are investigated and applied to broadening the operating bandwidth of antennas [12]–[15]; power amplifiers [16], [17]; or VCOs [5]. In [18], a fixed negative capacitor is used to enhance the varactor's TD. In general, these non-Foster elements are beneficial and can address the fundamental limitations of common passive networks. There are several network topologies that can realize a non-Foster element. However, active circuits such as negative impedance converters (NICs), negative impedance inverters (NIIs), and amplifier-based negative group delay (NGD) networks are most popular methods investigated theoretically and practically in the literatures [18]–[21].

In this paper, a novel varactorless technique for tuning frequency is deployed for the Clapp VCO network. This VCO structure employs a tunable negative capacitor (TNC) to achieve higher FTR as compared to the original Clapp LC VCO whose FTR mainly relies on the varactor's tuning capability. The FTR performance is known quantitatively as "total tuning dynamic (TTD)". By setting properly the maximum capacitance of the TNC, wideband operation can be achieved without the necessity of high tuning-range controlling component. The proposed VCO can yield much higher TTD than that in the conventional one and can overcome the existing FTR limitation of the varactor-based method, even if the TNC's tuning capability is inferior to the varactor. For circuit implementation, the TNC is realized by a negative impedance inverter (NII) which the gate voltages of cross-coupled dual transistors control the negative capacitance. The simulation results of the overall VCO network with the realized TNC based on discrete components have proven the advantage of the proposed method with TTD over TD of the TNC. The practical VCO applications is feasible with acceptable phase noise performance.

The rest of the paper is organized as follows: section II presents proposed technique with analytical demonstrations and validations based on an ideal TNC. Then, the circuit realization of the TNC and the overall VCO implementation are discussed in section III. Section IV shows simulation results that prove the advantages of the proposed VCO network. Discussions and conclusion are finally made in section V and section VI, respectively.

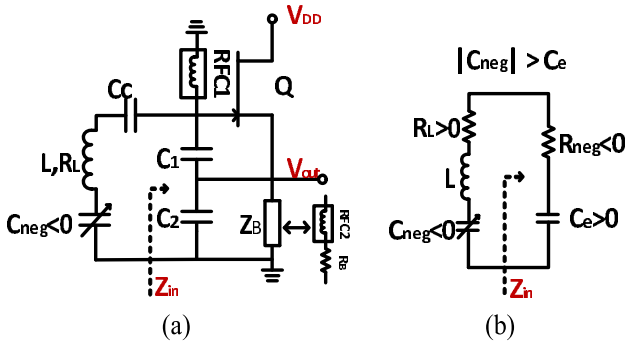

FIGURE 1. (a) Proposed Clapp VCO structure with a tunable negative capacitor (C_{neg} is substituted by a varactor in the conventional Clapp VCO [1]). (b) small-signal AC equivalent model.

II. LC-TANK VCO DESIGN WITH VARACTORLESS FREQUENCY-TUNING TECHNIQUE

A. USING A TNC TO INCREASE FTR

The proposed Clapp VCO structure is shown in Fig 1(a) which employs varactorless frequency-tuning method. In this network, active device Q, typically junction field-effect transistor (JFET), is configured in the common-drain mode with DC biasing network consisting of a shunt RF choke (RFC1) at the gate and components Z_B (a series connection of a resistor and a RF choke RFC2). A voltage-controlled negative capacitor is utilized to sweep oscillation frequency instead of the conventional varactor. Fig 1(b) shows equivalent VCO model in the non-parasitics small-signal analysis [1] with impedance Z_{in} exhibiting a series connection of a negative resistor R_{neg} and a positive equivalent capacitor C_e which are given as follows:

$$R_{neg} = \frac{-g_m}{\omega^2 C_1 C_2}, \tag{1}$$

$$C_e = \frac{C_1 C_2}{C_1 + C_2}, \tag{2}$$

where g_m denotes small-signal transconductance at the biasing point of the transistor, $|R_{neg}|$ decreases with the increase of oscillation frequency, and C_e is independent of g_m. To make VCO oscillate, the resistance value R_{neg} must satisfy the start-up condition, i.e., $|R_{neg}| > R_L$, in order to compensate completely for the inductor loss R_L. Then, the transconductance g_m will be reduced in large-signal regime leading to $|R_{neg}| = R_L$, and the steady-state oscillation is sustained with frequency

$$f_{osc} = \frac{1}{2\pi\sqrt{L\left(\dfrac{C_{neg}C_e}{C_{neg}+C_e}\right)}}. \tag{3}$$

In the common wideband LC VCOs, the frequency range is covered by the ratio f_{max}/f_{min} which is proportional to the root of the total capacitance ratio $C_{t,max}/C_{t,min}$ in the LC tank:

$$D_t = \frac{C_{t,max}}{C_{t,min}} = \left(\frac{f_{max}}{f_{min}}\right)^2, \tag{4}$$

where D_t is referred as the TTD of the VCO network. In order to showcase effectiveness of the proposed structure in increasing the VCO FTR, the conventional Clapp VCO using a positive-capacitance varactor with the TD of $D = C_{var,max}/C_{var,min}$ for tuning is taken into account for comparison. Then, the series association of C_e and C_{var} results in the total capacitance as follows:

$$C_t = \frac{C_e C_{var}}{C_e + C_{var}}. \tag{5}$$

With the varactor tuning range from $C_{var,min}$ to $C_{var,max}$, the TD of C_t or the TTD of the VCO is then written as

$$\begin{aligned} D_t &= \frac{C_{t,max}}{C_{t,min}} = \frac{C_e + C_{var,min}}{C_e + C_{var,max}} \times \frac{C_{var,max}}{C_{var,min}} \\ &= k \times D, \end{aligned} \tag{6}$$

where $k = (C_e + C_{var,min})/(C_e + C_{var,max})$. It is clear that because $0 < C_{var,min} < C_{var,max}$, k is always less than 1 and then $D_t < D$. The FTR performance is apparently restrained to the varactor tuning. Therefore, in order to obtain a wide operating VCO bandwidth, the only method is to deploy a varactor with high-TD capability. On the other hand, a negative capacitor can yield the total capacitance C_t as follows

$$C_t = \frac{C_e C_{neg}}{C_e + C_{neg}}. \tag{7}$$

From (7), we must take $|C_{neg}| > C_e$ in order to obtain the positive net capacitance. Assuming that the negative capacitor can sweep its capacitance amongst $C_{neg,min}$ and $C_{neg,max}$ with TD $D' = C_{neg,min}/C_{neg,max}$, the TD of C_t is then calculated by

$$\begin{aligned} D_t &= \frac{C_{t,max}}{C_{t,min}} = \frac{C_e + C_{neg,min}}{C_e + C_{neg,max}} \times \frac{C_{neg,max}}{C_{neg,min}} \\ &= \frac{1 + k'/D'}{1 + k'}, \end{aligned} \tag{8}$$

where $k' = C_e/C_{neg,max}$, $D' > 1$ and $-1 < k' < 0$. According to (8), D_t depends on both k' and D'. When k' goes to -1 or $|C_{neg,max}|$ is close to C_e, D_t can reaches very high value for any values of D'. Therefore, this can reduce the tuning-range requirement for the tuning component by focusing on assigning its maximum capacitance.

For the sake of comparison convenience, with the same TD, i.e., $D = D'$, our proposed VCO can provide high TTD, at least over the tuning component's TD, if $|C_{neg}| > C_e$ and $|C_{neg,max}|$ is close enough to C_e, while the tuning range of the varactor-based VCO is always limited to the tuning capability of the varactor.

B. VALIDATION WITH IDEAL TNC

To validate the above analysis, a simulation VCO schematic is generated using Advanced Design Software (ADS) with a realistic discrete transistor NE33284A whose I-V characteristic is described in Fig. 2. The oscillation frequency is expectedly within a range of 500 – 1300 MHz. The transistor

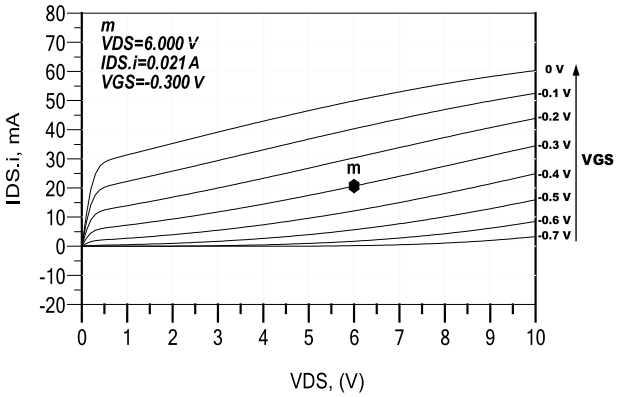

FIGURE 2. I-V characteristic of NE33284A.

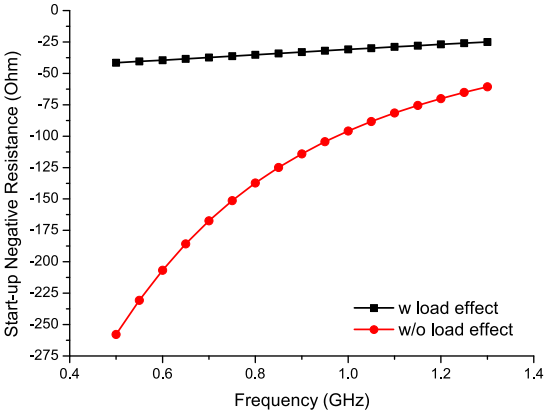

FIGURE 3. Start-up negative resistance for with and without load effect.

operates at the biasing point m of $21mA$ and $6V$ for drain current I_{DS} and voltage V_{DS}, respectively, leading to the biasing resistance $R_B = 12\Omega$ and the supply voltage $V_{DD} = 6.2V$. The capacitance values of the capacitors C_1, C_2 are equally $3.2pF$, and the parasitic resistance R_L is assumed 0.1Ω which is common in the high-Q off-chip inductors. It is noted that the output VCO signal can be terminated by a buffer amplifier to avoid loading effect. Nevertheless, in our work, a 50Ω load is used to terminate the output signal due to its simplicity and power non-consuming property, while the start-up condition ($|R_{neg}| > R_L$) is still satisfied.

Using S-parameter simulation, the start-up (small-signal) parameters in cases of with and without 50Ω termination, i.e., R_{neg} and C_e, are extracted over the frequency range of 500 – 1300 MHz and shown in Fig. 3. With load effect, the negative resistance is lower than that in case of without load effect. However, both of scenarios satisfy the start-up condition, i.e., $R_{neg} > R_L = 0.1\Omega$, which can trigger an oscillation. Unlike the non-parasitics extraction in (2), the start-up equivalent capacitance C_e varies slightly from $1.28pF$ to $1.57pF$ which can be seen in Fig. 4. Note that these parameters are in small-signal regime. Since the output VCO signal gradually becomes saturated with higher power, the effect of the transistor parasitics and package can lead to change in C_e and then resonant frequency. Therefore, it is important to

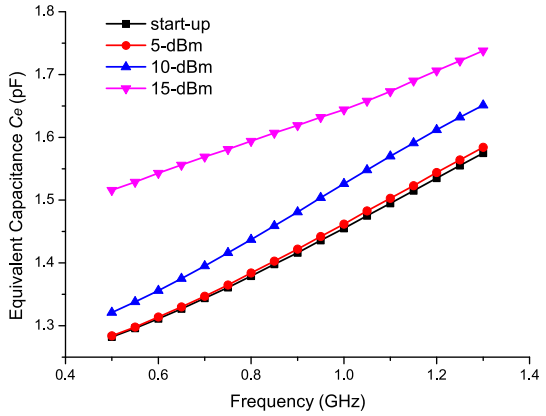

FIGURE 4. Equivalent capacitance C_e over different signal-power levels.

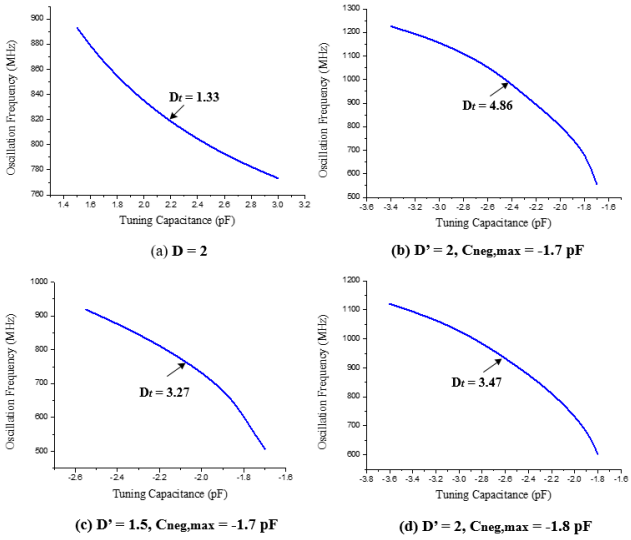

FIGURE 5. Oscillation frequency range for several scenarios of the tuning component: (a) ideal varactor. (b-d) ideal TNC.

consider C_e at the saturated-signal power to select appropriately the maximum TNC capacitance. In Fig. 4, C_e increases with the increase of signal power. For example, the maximum value of C_e goes from $1.57pF$ at the start-up level to $1.68pF$ at the 10-dBm signal level. Then, in order for our proposed VCO network to operate properly in the bandwidth with the $\leq$ 10-dBm power, the maximum TNC capacitance must be set so that $|C_{neg,max}| > 1.68pF$. The resonant inductance L also needs to be adjusted correctly to drop oscillation frequency in that bandwidth.

Fig. 5 shows FTR performance for several different tuning cases, i.e., an ideal TNC for the proposed structure and an ideal positive-capacitance varactor for the conventional Clapp structure. Those ideal tuning components are assumed to exhibit flat capacitance over an infinite bandwidth.

It can be seen that for a varactor with $D = 2$, the VCO only yields an oscillation bandwidth of 120 MHz, exhibiting $D_t = 1.33$ units which is less than the varactor TD. In contrast, using a TNC with the same TD, i.e., $D' = D = 2$, and its maximum negative capacitance is set at $-1.7pF$, satisfying $|C_{neg}| > C_e$ within the considerable bandwidth, the TTD of 4.86 units is much higher than the TD of the tuning component, corresponding a bandwidth of 690 MHz. In addition, even with the lower TD of the TNC, compared to the varactor, our proposed network can still provide a higher TDD as shown in Fig. 5c. Fig. 5d shows a TNC case with $D' = 2$ and lower maximum capacitance $C_{neg,max} = -1.8pF$. It confirms that higher difference between $|C_{neg,max}|$ and C_e leads to lower VCO TDD as well as narrower oscillation bandwidth.

In general, the TNC-based tuning method can benefit VCO FTR performance which depends not only on the TNC's TD, but its maximum capacitance.

III. VCO IMPLEMENTATION WITH NON-IDEAL TNC

The advantageous operation of the proposed tuning method based on a TNC has been validated but the TNC does not naturally exist as varactors, inductors, capacitors, or transistors. Therefore, in this section, the realization of the TNC as well as the proposed VCO is carried out that can exhibit the expected operation.

A. TNC REALIZATION

Apparently, with a variable non-Foster capacitor, the VCO's bandwidth can be expanded remarkably by selecting the maximum negative capacitance close to the equivalent capacitance C_e. The practical design of this component is challenging and requires a particular network topology because of its natural inexistence. Some of the promising candidates for generating a high-Q non-Foster capacitor are based on negative impedance converters (NICs) [19], negative impedance inverters (NIIs) [18], or amplifier-combined negative group delay (GND) networks [16], [21]. However, not all can provide negative capacitance varying with respect to the controlling DC voltage in a linear manner that can be applicable to our VCO structure. Moreover, unlike an ideal non-Foster capacitor which can exhibit the negative capacitance in an infinite bandwidth, the generators of the non-Foster capacitors only operate correctly within a limited bandwidth due to the operating frequency limitation of their constituting elements. Therefore, the device selection is important to design a non-Foster circuit that can cover the required frequency range.

In this paper, the proposed VCO structure requires a TNC connected in shunt. Referring to NII in [18], a shunt negative capacitor can be realized with cross-coupled transistors as shown in Fig. 6a. Taking small-signal analysis and assuming the operating frequency is much smaller than the characteristic frequency given by [18]:

$$f_c = \frac{g_m^2 R_{ds}}{2\pi C_{gs}}, \tag{9}$$

where R_{ds} and C_{gs} are the transistor parasitics; the impedance Z_n is equivalently composed of three series negative elements as shown in Fig. 6b. The negative resistance R_n can be used

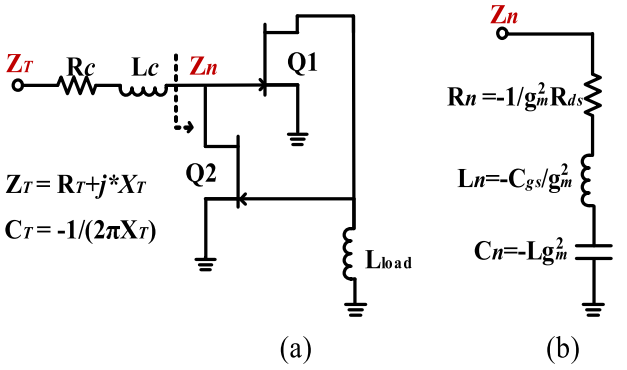

FIGURE 6. (a) NII structure for realizing a tunable negative capacitor. (b) small-signal equivalent model.

to increase start-up VCO gain or be negated by a positive resistor R_c to limit signal power, which will be discussed in next section. The component L_c, in contrast, must be inserted to compensate for L_n.

It can be seen that the negative capacitance depends on the JFET transconductance g_m which can be calculated from the Shockley's equation as follows:

$$g_m = \frac{-2I_{DSS}}{V_P}\left(1 - \frac{V_{GS}}{V_P}\right), \tag{10}$$

where V_P denotes the pinch-off voltage, and I_{DSS} is the maximum drain current and occurs as $V_{GS} = 0V$ and $V_{DS} = |V_P|$. By changing g_m, it is possible to obtain a range of the negative capacitance. This can be done by sweeping the transistor gate voltage V_{GS} according (10). However, the linear variation of C_n is difficult to be achieved because the parasitic elements also depend on the transistor transconductance g_m while the fixed element L_c only negate exactly the parasitic L_n at one value of g_m. As g_m varies, inductance difference between L_c and L_n will contribute to reactance due to C_n, devastating the linear variation of C_n. Also, the package elements of the discrete devices can partially influence the TNC's linearity.

In this work, the active devices with model NE33284A are selected to design a TNC with following datasheet-based parasitics: $R_{ds} \approx 200\Omega$, $C_{gs} \approx 0.22pF$ and $g_{m,min} \approx 20mS$, leading $f_{c,min} \approx 64$ GHz which much higher than the expected operating frequency within 500-1300 MHz. Therefore, it is possible to utilize this transistor model for TNC realization. The simulation responses of the TNC in small-signal regime are shown in Fig. 7 with $L_{load} = 1.3pF$, and $L_c = 1.6nH$. Two active transistors are biased at $V_{DS} = 8V$. It can be seen that the NII network can provide negative-capacitance response corresponding to the negative-slope positive reactance with frequency over the bandwidth. For each value of V_{GS} from $-0.6V$ to $0V$, the negative capacitance increases in an acceptable linear manner with the maximum value of about $-1.3pF$, which can be used to tune the oscillation frequency in the proposed VCO architecture.

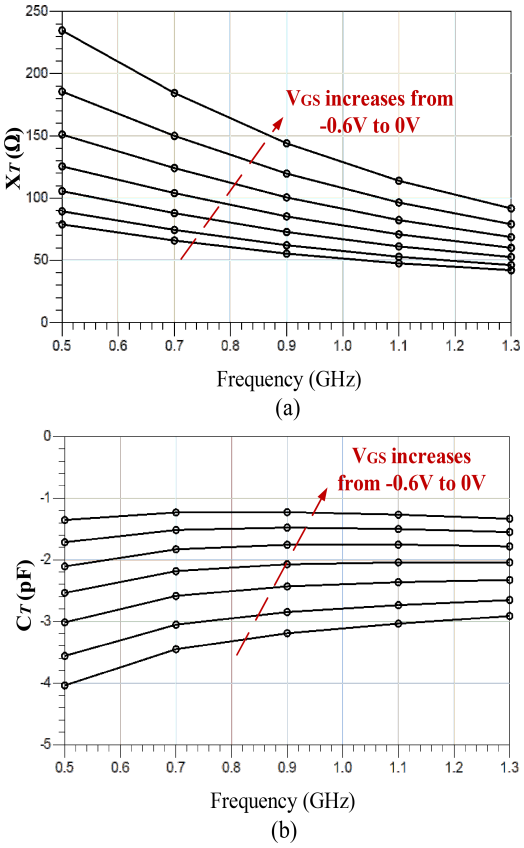

FIGURE 7. Responses of the realized TNC in small-signal regime: (a) reactance. (b) capacitance.

B. STABILITY EVALUATION OF TNC

One of main challenges in NIC or NII networks with cross-couped transistors is the instability problem that spurious oscillations occur without input signal causing additional power consumption and undesired behavior [20], [22]. These additional oscillations cannot be detected by small-signal simulation ADS tools which consider circuit responses in a short period. One of the popular stability-testing methods is to examine the reflection coefficient (S_{11}) contour of the overall circuit by using "OscTest" tool which is available in ADS. The number of clockwise encirclements of the point $1 + 0j$ denotes the number of oscillations in the circuit. Fig. 8 shows the S_{11} contour of the TNC which is, for example, connected to a 50Ω termination and biased at $V_{GS} = -0.3V$. It is clear that there are two instability encirclements crossing the x axis at 2.284 GHz and 10.16 GHz which denote the spurious oscillation frequencies as well as the instability of the TNC. Due to this problem, it is impossible to verify a separate TNC circuit, commonly connected to the 50Ω port of the network analyzers.

Nevertheless, the instability problem can be overcome by connecting an appropriate load network to it for "open-circuit stable" and "short-circuit stable" non-Foster network types or inserting notch filters into feedback branches [13], [14]. Another possible way is to isolate the output signal with

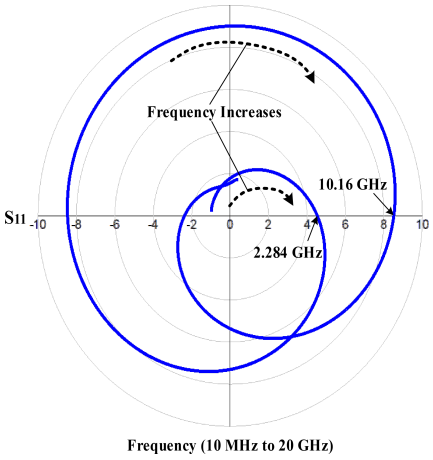

FIGURE 8. Instability behavior of the TNC biased at $V_{GS} = -0.3$V and connected with a 50Ω termination.

a buffer amplifier, then remove additional oscillations by band-pass filters. In this research, the non-Foster element is embedded to the VCO network, not a 50Ω termination. Therefore, it is better to carry out a stability-checking process in the TNC-combined network. The overall VCO circuit is stable if there is only an oscillation frequency and its harmonics in the spectrum.

C. OVERALL VCO IMPLEMENTATION

In this subsection, an overall VCO network with a non-ideal TNC is implemented and verified. With the same components of the VCO core assigned in section IIB, our proposed circuit requires to design a large-signal broadband TNC that the magnitude of its maximum capacitance is greater than $1.68pF$ due to the estimated signal power of about 10 dBm, while remaining high-enough quality (Q) factor to ensure the start-up condition. In essence, each tuning voltage or negative capacitance results in a resonant frequency. Therefore, exhibiting the required negative capacitance at its resonant frequency is sufficient for the TNC design.

TABLE 1. Optimal component parameters of the overall VCO network.

L	C_1	C_2	R_B	L_c	R_c	L_{load}	R_L
4.6nH	3.2pF	3.2pF	12Ω	1.6nH	22Ω	1.3pF	0.1Ω

It is possible to utilize the TNC design in Section III, substituting the ideal tuning component in the proposed VCO structure in Fig. 1a. However, this TNC is only investigated in small-signal regime that will turns to large-signal regime with smaller transconductance as the VCO signal becomes saturated. As a result, the large-signal TNC behavior is different from that shown in Fig. 7, and its small-signal linearity can no longer exist. Fortunately, the tuning linearity of the TNC can be remained by suppressing signal to a small-enough level. Therefore, a component-tuning scheme is useful in the overall network to obtain the desired performance.The overall VCO network is shown in Fig. 9 and Table 1 lists its final optimal values of components after tuning process.

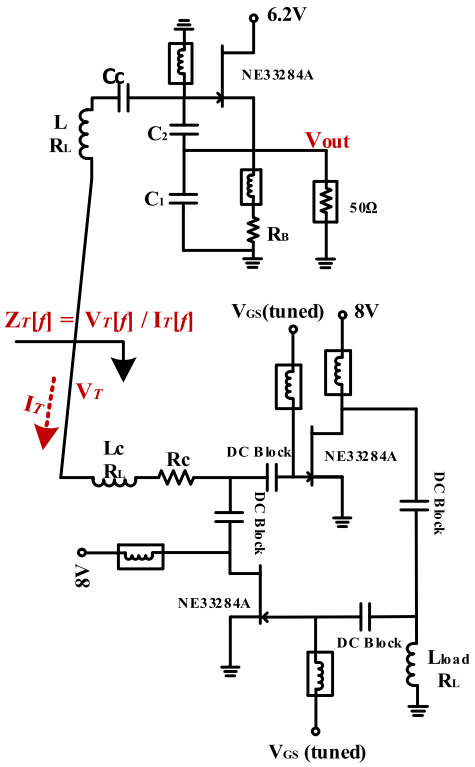

FIGURE 9. Overall VCO structure with non-ideal TNC and biasing networks.

The compensation resistor $R_c = 22\Omega$ is necessarily utilized so as to reduce negative resistance or start-up VCO gain, restraining signal power to ensure the linear variation of the non-Foster capacitance as close as that considered in the small-signal analysis. The common inductors are supposed to exhibit very-small parasitic resistance 0.1Ω due to their off-chip property.

IV. SIMULATION RESULTS

Using "OscTest" element in ADS to check the oscillation capability as well as the stability of the overall circuit, Fig. 10 shows S_{11} contours at several cases of V_{GS}. It can be seen that the x axis value of 1.0 is circled clockwisely by the $S11$ contour as the frequency increases, denoting that the circuit oscillates. The point on the trace where it crosses the x axis can predict quasi-exactly oscillation frequency. Moreover, there is no more clock-wise encirclement of the $1 + j0$ point indicating that the VCO circuit is stable with only a right-hand plane (RHP) pole produced due to the feedback. Therefore, no additional effort is necessarily required to stabilize the VCO circuit while the current drawn by DC sources is minimized leading to minimal power consumption. Then, the tuning capacitance of the negative capacitor at an oscillation frequency f is extracted in large-signal regime as follows

$$C_T[f] = \frac{-1}{2\pi Z_T[f]}, \tag{11}$$

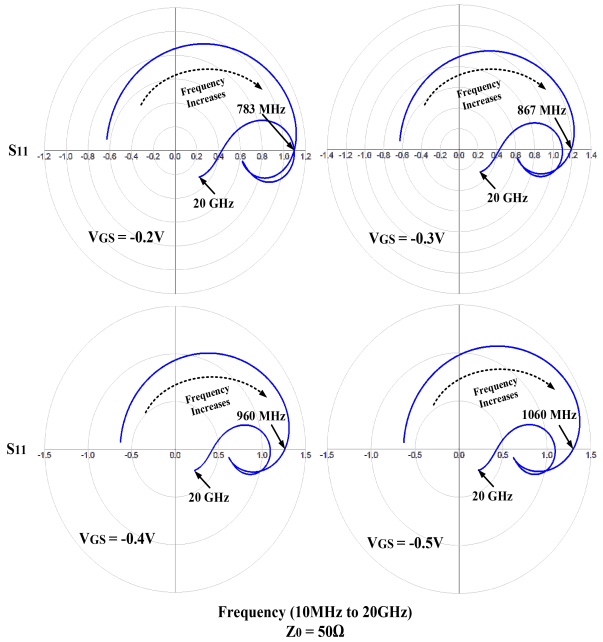

FIGURE 10. Oscillation and stability tests of the overall VCO structure at several values of the controlling voltage V_{GS}.

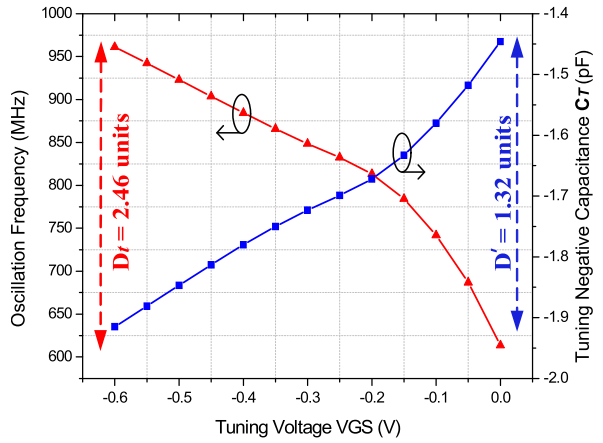

FIGURE 11. Extracted performance of the overall VCO network: total tuning dynamic D_t and tuning dynamic of the non-Foster tuning component D'.

where

$$Z_T[f] = \text{Imag}\left(\frac{V_T[f]}{I_T[f]}\right). \tag{12}$$

Note that the oscillation frequency f corresponds with the tuning voltage V_{GS}. By using "OscPort and ADS Harmonic Balance Simulation" tools, the FTR and the extracted tuning negative capacitance versus the controlling voltage V_{GS} are shown in Fig. 11. The frequency ranges from 614 to 961 MHz yielding a TTD of $D_t = 2.46$ units. With each tuning voltage value, the tuning negative capacitance C_T extracted varies from $-1.92pF$ to $-1.45pF$, corresponding a TD of $D' = 1.32'$ units which is less than the TTD, confirming the advantageous operation of the Clapp VCO with the proposed tuning method. The maximum capacitance of $-1.45pF$ which is slightly higher than the required one of $< -1.68pF$

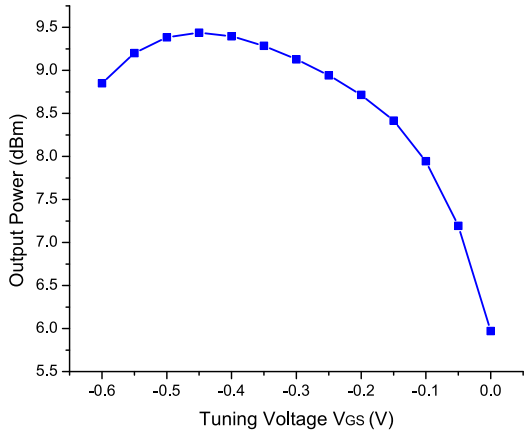

FIGURE 12. Output signal power over different tuning voltages.

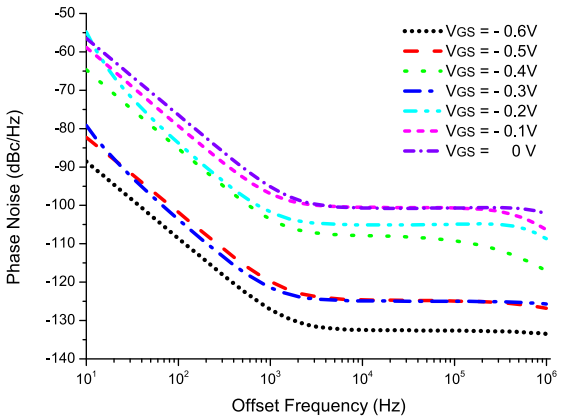

FIGURE 13. Simulation phase noise performance.

is because the saturated power at $V_{GS} = 0V$ is only 6 dBm shown in Fig. 12 with the corresponding oscillation frequency of < 1 GHz. Then, the equivalent C_e is about 1.42 pF which can be determined in Fig. 4.

In addition, the VCO output power varies by only about 3.5 dBm between 6 and 9.5 dBm. The power difference mainly stems from the real-part discrepancy of the impedance induced by the TNC over the overall bandwidth. Fig. 13 shows VCO phase noise performance at each oscillation frequency. It can be seen that phase noise is saturated at offset frequency of 2 kHz with below -95 dBc/Hz for every value of tuning voltage. At 1 MHz offset frequency, the phase noise performance is slightly improved with <-100 dBc/Hz.

V. DISCUSSIONS

A. EXTEND TO PARALLEL ASSOCIATION

The proposed tuning method can be extended to a parallel connection between the TNC and the equivalent capacitor C_e. Then, the TTD is rewritten as follows:

$$D_t = \frac{C_e + C_{neg,max}}{C_e + C_{neg,min}}. \tag{13}$$

It is clear that if $|C_{neg}| < C_e$ and $C_{neg,min}$ is close to C_e, D_t can similarly reach to very high value. However, this parallel association is difficult to deploy in the Clapp structure due

TABLE 2. Performance comparison among state-of-the-art VCOs.

Reference	FTR (GHz)	V_{tune} (V)	Phase Noise @1MHz (dBc/Hz)	FOM	FOMT	Tuning Method
[10]	1.78-1.95 (10%)	1∼2.7	-105 ∼ -115	157∼166	157∼166	Varactorless/Voltage-Controlled Inductor
[5]	3.8-5.2 (31%)	0∼2	-109 ∼ -110	171∼176	181∼186	Varactorless/Tunable Negative Inductor
[24]	2.49-3.17 (24%)	0∼1.2	-102 ∼ -111	156∼170	163∼178	Varactorless/Transformer-Based Technique
[25]	5.1-6.1 (17.9%)	-1.8∼1.8	-111 ∼ -113	177∼180	182∼185	Varactor/Oppositely-Aligned Varactor
[26]	3.1-5.2 (51%)	0∼1.2	-115 ∼ -119	179∼185	193∼199	Varactor/Varactor Array
This Work	0.61-0.96 (44%)	-0.6∼0	-101 ∼ -133	127∼167	140∼180	Varactorless/Tunable Negative Capacitor

to non-isolated C_e and more suitable in the differential LC VCOs [5].

B. DISCRETE AND INTEGRATED CIRCUIT IMPLEMENTATION

The VCO with the proposed tuning method has been realized using common discrete components and its advantageous operation has been proven by the simulation results. In the integrated circuit design, it is difficult to design inductors with high Q factor which is much lower than that of the off-chip inductors and main contributor to phase-noise performance degradation. However, these losses can be compensated by additional negative resistance from the TNC cell through reducing the compensation resistor R_c. Moreover, with good matching among components and without package effects, the linearity of tuning component can be improved.

C. PERFORMANCE EVALUATION

Our purpose of this paper is to apply a novel tuning method to the LC VCOs, specifically a JFET-based Clapp structure and verify its operation superior to the varactor-based one in terms of TTD relative to tuning component's TD in the discrete circuit implementation. Although the FTR is improved, but the proposed VCO is also required to exhibit tolerable phase noise as well as power consumption across different oscillation frequencies. The commonly used figure of merit (FOM) to evaluate the overall VCO performance is defined as follows:

$$FOM = -L(\Delta f) + 20log\frac{f_{osc}}{\Delta f} - 10log\frac{P_{DC}}{1mW}, \qquad (14)$$

where Δf and f_{osc} are the offset frequency and oscillation frequency in hert, respectively. $L(\Delta f)$ is the phase noise in dBc/Hz at Δf and P_{DC} is the power consumption in mW from both the VCO core and TNC cell. In order to account for the FTR (in percent), another parameter (FOMT) is introduced as [23].

$$FOMT = FOM + 20log\frac{FTR}{10}. \qquad (15)$$

Two parameters FOM and FOMT are used to only point that the proposed VCO can provide an acceptable overall performance in comparison with the existing works. Fig. 14 shows the FOM and FOMT performances over oscillation frequencies. The addition of a TNC increases the total power consumption, then leading to reduction in FOM and FOMT. At lower frequencies regarding to the higher gate voltages,

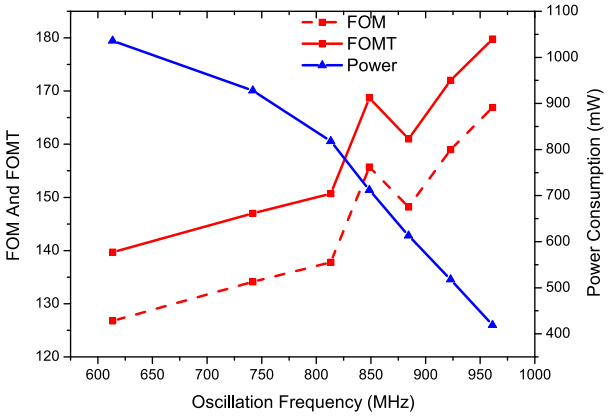

FIGURE 14. FOM and FOMT performance and power consumption of the VCO over oscillation frequency band.

the drain current increases and it is understandable with significant drop in FOM and FOMT at these frequencies. Compared to other state-of-the-art VCOs summarized in Table 2, the proposed VCO can exhibit similar phase noise with acceptable FOMT performance.

D. HIGHER FTR PERFORMANCE

Although the VCO FTR is significantly improved by designing the maximum capacitance magnitude of the TNC close to the equivalent capacitance C_e, the FTR performance is also depended on the tuning capacity of the tuning component according to (8). Therefore, it is possible to increase more FTR with higher g_m range of the active devices in the TNC cell. It can be seen from Table 2 that the tuning voltage of our proposed VCO is only from −0.6V to 0V which is much narrower than in other VCOs due to the V_{GS}-range limitation of the device NE33284A.

E. USING VARACTOR AND FIXED NEGATIVE CAPACITOR

The principle of the proposed tuning method can be switched to a series or parallel association of a varactor and a fixed negative capacitor. For example, if the total capacitance is a series connection of C_e, C_{var}, and C_{neg}, then D_t can be calculated as

$$D_t = \frac{C_{evar,max}}{C_{evar,min}} \times \frac{C_{evar,min} + C_{neg}}{C_{evar,max} + C_{neg}}, \qquad (16)$$

where $C_{evar} = C_eC_{var}/(C_e + C_{var})$. It can be seen that if satisfying the positive total capacitance condition, i.e., C_{evar}<|C_{neg}|, then the small difference between

$C_{evar,max}$ and $|C_{neg}|$ can lead to high value of D_t. However, the additional varactor can make the overall circuit more complicated and less effective at high frequency.

VI. CONCLUSION

A novel technique for tuning without varactors using a TNC has been deployed in the JFET-based Clapp VCO design. This method is flexible in which the maximum TNC capacitance can be adjusted to obtain high TTD performance over the TD of the tuning element, compared to the conventional Clapp VCO whose TTD is always limited to the varactor tuning capacity. This advantageous operation is successfully verified in the discrete-circuit implementation with the non-ideal TNC realized based on a shunt NII structure. In general, this proposed tuning method has potential to deploy in any LC VCO configurations and can provide a wider operating bandwidth by using the TNC-in active devices with higher tuning capability.

REFERENCES

[1] V. V. Ulansky, M. S. Fituri, and I. A. Machalin, "Mathematical modeling of voltage-controlled oscillators with the colpitts and clapp topology," *Electron. Control Syst.*, vol. 1, no. 19, pp. 82–90, Jun. 2009.
[2] D. M. Pozar, "Oscillators and mixers," in *Microwave Engineering*. Hoboken, NJ, USA: Wiley, Nov. 2011, pp. 604–627.
[3] R. Aparicio and A. Hajimiri, "A noise-shifting differential Colpitts VCO," *IEEE J. Solid-State Circuits*, vol. 37, no. 12, pp. 1728–1736, Dec. 2002.
[4] C. O'Connor, "Develop a trimless voltage-controlled oscillator," *Microw. RF*, vol. 39, pp. 94–105, Jan. 2000.
[5] Y. Chen and K. Mouthaan, "Wideband varactorless *LC* VCO using a tunable negative-inductance cell," *IEEE Trans. Circuits Syst. I, Reg. Papers*, vol. 57, no. 10, pp. 2609–2617, Oct. 2010.
[6] A. D. Berny, A. M. Niknejad, and R. G. Meyer, "A 1.8-GHz LC VCO with 1.3-GHz tuning range and digital amplitude calibration," *IEEE J. Solid-State Circuits*, vol. 40, no. 4, pp. 909–917, Apr. 2005.
[7] A. Kral, F. Behbahani, and A. A. Abidi, "RF-CMOS oscillators with switched tuning," in *Proc. IEEE Custom Integr. Circuits Conf.*, May 1998, pp. 555–558.
[8] J. Kim, J. Shin, S. Kim, and H. Shin, "A wide-band CMOS LC VCO with linearized coarse tuning characteristics," *IEEE Trans. Circuits Syst. I, Reg. Papers*, vol. 55, no. 5, pp. 399–430, May 2008.
[9] K. Kwok and J. R. Long, "A 23-to-29 GHz transconductor-tuned VCO MMIC in 0.13μm CMOS," *IEEE J. Solid-State Circuits*, vol. 42, no. 12, pp. 2878–2886, Dec. 2007.
[10] P. Andreani, "A 1.8-GHz monolithic CMOS VCO tuned by an inductive varactor," *Proc. ISCAS*, May 2001, pp. 714–717.
[11] R. M. Foster, "A reactance theorem," *Bell Syst. Tech. J.*, vol. 3, no. 2, pp. 259–267, Apr. 1924.
[12] Q. Tang and H. Xin, "Stability analysis of non-Foster circuit using normalized determinant function," *IEEE Trans. Microw. Theory Techn.*, vol. 65, no. 9, pp. 3269–3277, Sep. 2017.
[13] S. E. Sussman-Fort and R. M. Rudish, "Non-Foster impedance matching of electrically-small antennas," *IEEE Trans. Antennas Propag.*, vol. 57, no. 8, pp. 2230–2241, Aug. 2009.
[14] A. M. Elfrgani, R. Moussounda, and R. G. Rojas, "Stability assessment of non-Foster circuits based on time-domain method," *IET Microw., Antennas Propag.*, vol. 9, no. 15, pp. 1769–1777, Dec. 2015.
[15] F. Albarracín-Vargas, E. Ugarte-Muñoz, V. González-Posadas, and D. Segovia-Vargas, "Sensitivity analysis for active matched antennas with non-Foster elements," *IEEE Trans. Antennas Propag.*, vol. 62, no. 12, pp. 6040–6048, Dec. 2014.
[16] D. Nguyen, C. Seo, and K. S. Park, "A high-efficiency design for 2.0-2.9 GHz 5-W GaN HEMT class-E power amplifier using passive Q-constant non-Foster network," *Microw. Opt. Technol. Lett.*, vol. 62, no. 2, pp. 615–624, Feb. 2020.
[17] S. Lee, H. Park, K. Choi, and Y. Kwon, "A broadband GaN pHEMT power amplifier using non-Foster matching," *IEEE Trans. Microw. Theory Techn.*, vol. 63, no. 12, pp. 4406–4414, Dec. 2015.
[18] S. Kolev, B. Delacressonniere, and J. L. Gautier, "Using a negative capacitance to increase the tuning range of a varactor diode in MMIC technology," *IEEE Trans. Microw. Theory Techn.*, vol. 49, no. 12, pp. 2425–2430, Dec. 2001.
[19] A. Larky, "Negative-impedance converters," *IRE Trans. Circuit Theory*, vol. 4, no. 3, pp. 124–131, Sep. 1957.
[20] J. G. Linvill, "Transistor negative impedance converters," *Proc. IRE*, vol. 41, pp. 725–729, Jun. 1953.
[21] H. Mirzaei and G. V. Eleftheriades, "Realizing non-Foster reactive elements using negative-group-delay networks," *IEEE Trans. Microw. Theory Techn.*, vol. 61, no. 12, pp. 4322–4332, Dec. 2013.
[22] S. D. Stearns, "Circuit stability theory for non-foster circuits," in *IEEE MTT-S Int. Microw. Symp. Dig.*, Jun. 2013, pp. 1–3.
[23] Y. Wachi, T. Nagasaku, and H. Kondod, "A 28 GHz low-phase-noise CMOS VCO using an amplitude-redistribution technique," in *IEEE Int. Solid-State Circuits Conf. (ISSCC) Dig. Tech. Papers*, Feb. 2008, pp. 482–630.
[24] D. Pi, B.-K. Chun, and P. Heydari, "A 2.5-3.2 GHz CMOS differentially-controlled continuously-tuned varactor-less LC-VCO," in *Proc. IEEE Asian Solid-State Circuits Conf.*, Nov. 2007, pp. 111–114.
[25] T. T. Ta, S. Kameda, T. Takagi, and K. Tsubouchi, "A 5 GHz band low noise and wide tuning range Si-CMOS VCO," in *Proc. IEEE Radio Freq. Integr. Circuits Symp.*, Jun. 2009, pp. 571–574.
[26] D. Hauspie, E.-C. Park, and J. Craninckx, "Wideband VCO with simultaneous switching of frequency band, active core, and varactor size," *IEEE J. Solid-State Circuits*, vol. 42, no. 7, pp. 1472–1480, Jul. 2007.

DANG-AN NGUYEN (Graduate Student Member, IEEE) received the degree from the School of Electronics and Telecommunications, Hanoi University of Science and Technology (HUST), Vietnam. He is currently pursuing the Ph.D. degree with Soongsil University, South Korea, where his major relates to microwave signal processing, radar systems, power amplifiers, and non-Foster circuits. He has three years' experience working as a Senior Member of the Signal Processing and Radio Communication Laboratory.

CHULHUN SEO (Senior Member, IEEE) received the B.S., M.S., and Ph.D. degrees from Seoul National University, Seoul, South Korea, in 1983, 1985, and 1993, respectively. From 1993 to 1995, he was with the Massachusetts Institute of Technology (MIT), Cambridge, MA, USA, as a Technical Staff Member. From 1993 to 1997, he was with Soongsil University, Seoul, as an Assistant Professor. From 1999 to 2001, he was with MIT, as a Visiting Professor. From 1997 to 2004, he was with Soongsil University, as an Associate Professor. Since 2004, he has been a Professor of electronic engineering with Soongsil University. He was the IEEE MTT Korea Chapter Chairman, from 2011 to 2014. He is currently the President of the Korean Institute of Electromagnetic Engineering and Science (KIEES) and the Dean of the Information and Telecommunications College, Soongsil University. He is the Director of the Wireless Power Transfer Research Center, supported by the Korean Government's Ministry of Trade, Industry and Energy, and the Director of the Metamaterials Research Center, supported by Basic Research Laboratories (BRL) through an NRF grant funded by the MSIP. He is the Director of the Center for Intelligent Biomedical Wireless Power Transfer supported by the National Research Foundation of Korea (NRF) grant funded by the MSIP. His research interests include wireless technologies, RF power amplifiers, and wireless power transfer using metamaterials.